STRUCTURE AND DYNAMICS OF TURBULENT FLOWS OVER HIGHLY PERMEABLE WALLS

Wim-Paul Breugem[1], Mehdi Niazi Ardekani [2] & Gerrit E. Elsinga[1]
[1]*Delft University of Technology, Laboratory for Aero and Hydrodynamics, Leeghwaterstraat 21, 2628 CA Delft, The Netherlands*
[2]*KTH Mechanics, Linné FLOW Centre, SE-100 44 Stockholm, Sweden*

Abstract Highly porous materials are found in various industrial applications and environmental flows. In previous studies it was found that a turbulent flow along a highly porous wall experiences a higher skin friction as compared to a solid wall with similar surface roughness when the so-called permeability Reynolds number (Re_K) is larger than $O(1)$. The main objective of the present study was to gain understanding of the characteristic structures and auto-generation mechanisms of turbulence for $Re_K \gg 1$. To this purpose the Volume-Averaged Navier-Stokes (VANS) equations were solved in a Direct Numerical Simulation (DNS) of a turbulent flow through a plane channel with an upper solid wall and a lower porous wall at $Re_K = 5.91$. The DNS results are in good agreement with available Particle Image Velocimetry (PIV) data for the same flow geometry. A linear stochastic estimation technique was used to capture the structure associated with the characteristic ejection event that contributes most to the Reynolds shear stress near the porous wall. This structure is similar to a horseshoe vortex. Contrary to the conventional hairpin vortex found near solid walls, this horseshoe vortex has a significantly higher inclination angle with the wall and its legs are much shorter. The latter is consistent with the observed absence of low and high-speed streaks near highly permeable walls. Next, the auto-generation mechanisms of the horseshoe vortex were studied in another DNS in which the horseshoe vortex was released in the Reynolds-averaged flow field obtained from the former DNS. Two distinct auto-generation mechanisms were observed: (1) the generation of new structures at the upstream end of the horseshoe vortex, which evolve rapidly into a turbulent spot with an arrowhead shape, and (2) the interaction of the horseshoe vortex with spanwise oriented Kelvin-Helmholtz vortex rollers originating from the inflexion point in the mean velocity profile near the porous wall.

INTRODUCTION

Turbulent flows over highly porous walls are encountered in several environmental processes and industrial applications such as flows over porous river beds, plant canopies, packed beds and metal foam heat exchangers. The permeability of such materials, i.e. the ability to transmit fluid through their pores, has a strong influence on the turbulent flow and hence on the skin friction and heat and mass transfer across the porous interface. In the laminar regime the skin friction is reduced by wall permeability due to an apparent slip velocity [1], while in the turbulent regime the skin friction is enhanced due to turbulent momentum transfer across the porous interface [2, 3, 4]. Breugem et al. [2] found that the effect of permeability depends on the so-called permeability Reynolds number, which is the ratio of the square root of the permeability (a measure for the effective pore size) to the viscous wall unit, $Re_K = \sqrt{K} u_\tau/\nu$. For $Re_K \ll 1$ a porous wall appears effectively impermeable to the turbulent flow, whereas for $Re_K \gg 1$ a porous wall behaves as a highly permeable wall near which viscous effects can be ignored. While turbulence near a solid wall is characterized by elongated low and high-speed streaks (regions of $u' < 0$ and $u' > 0$, respectively), it appeared that such structures are absent near highly permeable walls due to strong weakening of the wall-blocking effect [2, 5]. The objective of the present study was to gain more understanding of the change in structure and dynamics of turbulence near highly permeable walls, with a focus on the change in the auto-generation mechanisms of turbulence.

METHODOLOGY

Direct Numerical Simulations (DNS) were performed of a turbulent flow through a plane channel with an upper solid wall and a lower porous wall. The Volume-Averaged Navier-Stokes (VANS) equations were used to describe the macroscopic flow inside the porous wall layer [2]. The VANS equations reduce to the standard Navier-Stokes equations when the porosity is equal to 1 (no solids), while inside the porous layer an additional drag force from the solids appear in the momentum equations. The porosity, permeability and Forchheimer parameter of the isotropic porous layer were set to 0.8, 0.087 mm^2 and 0.027 s/mm, respectively, to enable comparison with Particle Image Velocimetry (PIV) data [3, 5] for turbulent channel flow over a ceramic foam plate. The dimensions of the channel were 6.5 H x 2.5 H x (H+H) in the streamwise, spanwise and wall-normal (porous layer + channel) direction, respectively. Periodic boundary conditions were applied in the streamwise and spanwise directions, while no-slip/no-penetration conditions were applied to the solid top wall and the solid bottom wall underneath the porous wall layer. The VANS equations were discretized on a Cartesian mesh with 384 x 288 x (128 + 192) cells in the streamwise, spanwise and wall-normal direction (porous layer + channel), respectively. The mesh was staggered and non-uniform in the wall-normal direction with the finest mesh around the porous interface and near the solid top wall ($\Delta x^+ = 10.2$, $\Delta y^+ = 5.2$ and $\Delta z^+ = 0.8 - 12.5$). Spatial gradients were computed from a pseudo-spectral method for the horizontal directions and the central-differencing scheme for the wall-normal direction. The VANS equations were integrated in time with a standard pressure-correction method. The flow was driven by a streamwise pressure-gradient such that the channel bulk Reynolds number remained constant at $Re_b = 5400$.

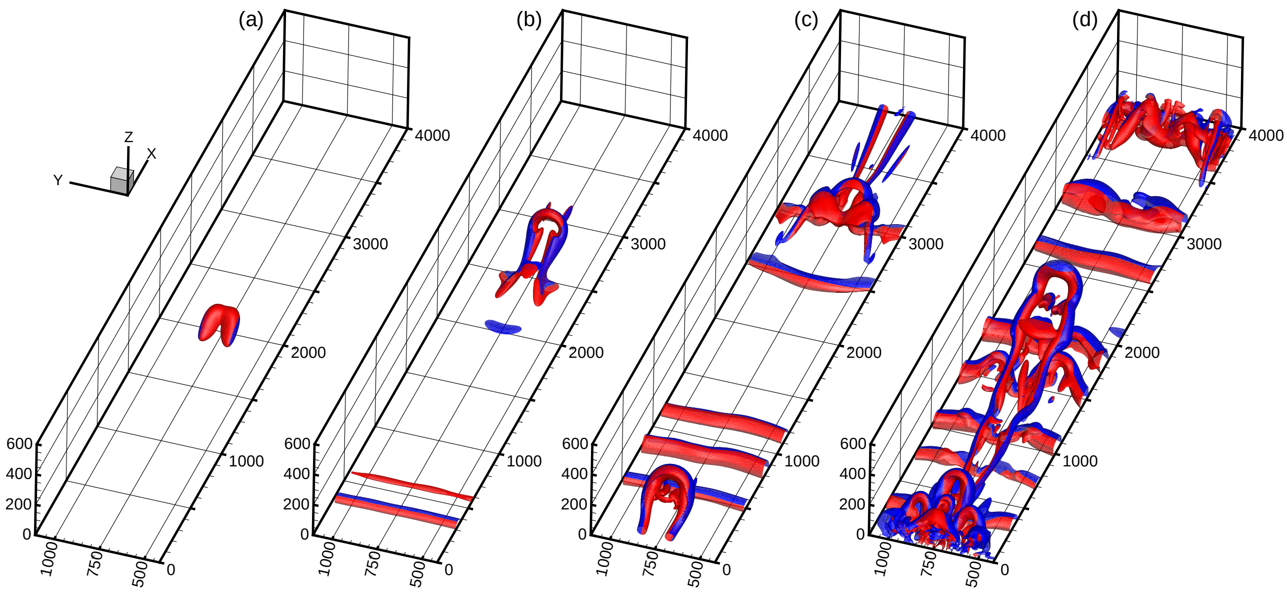

Figure 1. Temporal evolution of a conditional eddy associated with the characteristic ejection event that contributes most to the Reynolds shear stress at distance $z^+ = 75.7$ from the porous interface. The eddy strength is 2. The structures depict iso-surfaces of the so-called Q-criterion equal to 10% of the maximum Q-value at $t^+ = 0$. The iso-surfaces are colored by the sign of the wall-normal velocity fluctuation: red for upward and blue for downward motions. (a) $t^+ = 0$ (initial condition); (b) $t^+ = 133.7$; (c) $t^+ = 303.3$; (d) $t^+ = 467.3$.

RESULTS & DISCUSSION

From the DNS it was found that $Re_K = 5.91$, so the porous wall was highly permeable. This value is close to the value of 6.23 reported by Suga et al. [3]. Good agreement with the PIV data was also found for the mean velocity profile, the rms of the streamwise and spanwise velocity, and the Reynolds shear stress (not shown). A linear stochastic estimation technique [6] was used to extract the characteristic flow structure associated with the ejection event that contributes most to the Reynolds shear stress at a distance $z^+ = 75.7$ from the porous interface. This structure is depicted in Fig. 1a. Next, another DNS was performed in which this structure, or *conditional eddy*, was released in the Reynolds-averaged flow field obtained from the former DNS in order to study its temporal evolution, see Fig. 1a-d. The following observations were made. First, the conditional eddy is alike a horseshoe vortex. Contrary to the conventional hairpin eddies found near solid walls [6], this horseshoe vortex has a significantly higher inclination angle with the wall and its legs are much shorter; the latter is consistent with the observed absence of low and high-speed streaks near highly permeable walls [2, 5]. Second, spanwise oriented Kelvin-Helmholtz vortex rollers rapidly develop at the porous interface, which originate from the inflexion point in the mean velocity profile near the porous interface [2]. Third, after release of the conditional eddy soon new structures are created at its upstream end, which evolve rapidly into a turbulent spot with an arrowhead shape (this is clearly visible in Fig. 1d). Fourth, when the head of the horseshoe vortex travels over the Kelvin-Helmholtz vortex rollers, the spanwise oriented rollers rapidly evolve into horseshoe vortices with a streamwise orientation. This behavior is clearly different from the dynamics of hairpin vortices near solid walls [6].

References

[1] G.S. Beavers and D.D. Joseph. Boundary conditions at a naturally permeable wall. *J. Fluid Mech.* **30**:197-207, 1967.

[2] W.-P. Breugem, B.J. Boersma and R.E. Uittenbogaard. The influence of wall permeability on turbulent channel flow. *J. Fluid Mech.* **562**:35–72, 2006.

[3] K. Suga, Y. Matsumura, Y. Ashitaka, S. Tominaga and M. Kaneda. Effects of wall permeability on turbulence. *J. Heat Fluid Flow* **31**:974–984, 2010.

[4] A.F.E. Zagni and K.V.H. Smith. Channel flow over permeable beds of graded spheres. *J. Hydraul. Div.* **102**:207-222, 1976.

[5] K. Suga, M. Mori and M. Kaneda. Vortex structure of turbulence over permeable walls. *Int. J. Heat Fluid Flow* **32**:586-595, 2011.

[6] J. Zhou, R.J. Adrian, S. Balachandar and T.M. Kendall. Mechanisms for generating coherent packets of hairpin vortices in channel flow. *J. Fluid Mech.* **387**:353-396, 1999.